ACR Open Rheumatology
Vol. 7, No. 5, May 2025, e70033
DOI 10.1002/acr2.70033

American College of Rheumatology
Empowering Rheumatology Professionals

Gut Expansion of a Human Lupus Pathobiont is Associated With Autoantibody Production and T Cell Dysregulation

Longhuan Ma,[1] Yong Ge,[1] Natalie Six,[1] Seung-Chul Choi,[1] Josephine Brown,[2] Abigail Castellanos Garcia,[1] Mansour Mohamadzadeh,[1] Gregg J. Silverman,[3] and Laurence Morel[1]

Objective. The mechanisms by which the gut microbiome contributes to lupus pathogenesis remain poorly understood. The anaerobe *Ruminococcus gnavus* (*RG*) expands in patients with lupus in association with flares. The goal of this study was to determine the mechanisms by which candidate pathobiont lipoglycan-producing *RG2* may contribute to autoimmunity and to identify factors promoting its expansion.

Methods. The consequences of *RG* colonization or depletion were evaluated in the B6.*Sle1.Sle2.Sle3* triple congenic (TC) lupus model by flow cytometry and enzyme-linked immunosorbent assay. *RG* lysates were tested on Treg cells in vitro. Fecal microbiota transfers evaluated the contribution of the microbiome origin from lupus or control donors and dietary tryptophan. *RG1* and *RG2* growth and metabolome were evaluated in response to tryptophan in vitro.

Results. Only *RG2* stably colonized TC mice, in which it induced autoantibody production and T cell activation. Depletion of anaerobes had the opposite effect, with an increased Treg frequency. *RG2* induced Treg apoptosis in cocultures with dendritic cells. *RG* is present in TC microbiota, from which it is amplified by tryptophan. The combination of TC microbiota and high dietary tryptophan induced autoimmune activation and intestinal inflammation in healthy control mice. Finally, tryptophan enhanced *RG2* growth and production of immunomodulatory metabolites.

Conclusion. *RG2* contributes to autoimmune activation, at least by inducing Treg apoptosis. The expansion of this pathobiont is promoted by host genetic factors and tryptophan metabolism. Thus, targeted *RG2* depletion may improve disease outcomes in patients with lupus.

INTRODUCTION

Systemic lupus erythematosus (SLE) has been closely associated with gut microbial dysbiosis in patients and in mouse models of the disease.[1] Multiple mechanisms have been proposed to contribute to pathogenesis, including decreased microbial community richness and diversity. Specific microbial taxa, such as *Lactobacillus reuteri*[2] and *Enterococcus gallinarium*,[3] have been shown to induce autoimmune phenotypes in lupus-prone mice, although their greater relevance to clinical disease remains controversial. In patients with lupus, an increased fecal abundance of *Ruminococcus (blautia) gnavus* (*RG*) is positively correlated with disease severity, especially in those with active lupus nephritis (LN).[4] Longitudinal studies have shown that *RG* intestinal blooms occur during disease flares.[5] Moreover, *RG* strains isolated during these flares were found to produce a structurally novel, highly immunogenic lipoglycan (LG), and, in these patients, high titers of serum anti-LG IgG directly correlated with disease activity.[5] Colonization of nonautoimmune mice with LG-expressing *RG* strains, but not an *RG* strain without LG-expression, induced the production of anti-LG antibodies and lupus autoantibodies and impaired the intestinal mucosal barrier.[6] *RG* is a commensal found in healthy human microbiota, but its expansion has been disproportionally associated with diseases of the gut and other inflammatory conditions that now include SLE.[7] However, these studies have been correlative, without evidence that RG strains play

Supported by the NIH (grant R01-AI-143313 to Drs Ma and Silverman). The Flow Cytometry Shared Resource at University of Texas Health San Antonio is supported by a grant from the National Cancer Institute, NIH (P30-CA-054174) to the Mays Cancer Center, a grant from the Cancer Prevention and Research Institute of Texas (RP210126), and a grant from the NIH (S10-OD-030432), both awarded to Michael Berton, core director.

[1]Longhuan Ma, PhD, Yong Ge, PhD, Seung-Chul Choi, PhD, Natalie Six, Abigail Castellanos Garcia, MS, Mansour Mohamadzadeh, PhD, Laurence Morel, PhD: University of Texas Health San Antonio; [2]Josephine Brown, PhD: University of Florida, Gainesville; [3]Gregg J. Silverman, MD: New York University Grossman School of Medicine, New York.

Drs Ma and Ge are co-first authors and contributed equally to this work.

Additional supplementary information cited in this article can be found online in the Supporting Information section (http://onlinelibrary.wiley.com/doi/10.1002/acr2.70033).

Author disclosures are available at https://onlinelibrary.wiley.com/doi/10.1002/acr2.70033.

Address correspondence via email to Gregg J. Silverman, MD, at gregg.silverman@nyulangone.org; or to Laurence Morel, PhD, at morel@uthscsa.edu.

Submitted for publication March 17, 2025; accepted in revised form March 18, 2025.

a causative role in disease initiation or amplification. In particular, the mechanisms responsible for *RG* expansion in patients with SLE, as well as the causal consequences that this expansion has for the host immune system, are unknown.

To investigate the role of the gut microbiome in lupus pathogenesis, we used the B6.*Sle1*.*Sle2*.*Sle3* triple congenic (TC) model of lupus that does not inherently display altered gut barrier functional permeability.[8] Fecal microbiota transfers (FMTs) from TC mice with active disease into nonautoimmune C57BL/6 (B6) mice induced autoimmunity associated with a skewed tryptophan (Trp) metabolism linked to gut bacterial biochemical pathways.[9,10] In TC mice, high dietary Trp accelerated lupus pathogenesis, whereas low dietary Trp–induced expansion of FoxP3$^+$ CD4$^+$ regulatory Treg cells delayed disease progression.[9] Varying the level of dietary Trp also altered the gut microbiome of TC relative to B6 mice. These findings suggest that, besides a direct effect on immune cells, Trp could exert immunomodulatory influences by skewing the composition of the microbiota. These findings are of great potential clinical relevance because altered Trp metabolism has been reported in the serum, immune cells, and fecal samples of patients with SLE, with metabolomic shifts correlated with disease activity.[11] Moreover, several studies have reported that *RG* alters the host Trp metabolism with the production of metabolites that modulate the immune system and the gut–brain axis.[7]

Herein, we investigated the causal interactions between *RG* and autoimmune pathogenesis in a mouse model of lupus. *RG* fecal abundance naturally increases with age in TC but not in B6 mice, in correlation with the production of inflammatory cytokines. Oral gavages of the LG-producing *RG* strain only successfully colonized TC mice, in which it accelerated immune activation and autoantibody production. On the other hand, treatment of TC mice with metronidazole, which depletes most anaerobes, including *RG*, decreased the production of autoantibodies and increased the frequency of Treg cells that can suppress autoimmune disease. We found that lysates from the LG-producing *RG* strain induced apoptosis of Treg cells through interactions with dendritic cells (DCs). Following FMT into B6 recipients, high dietary Trp enriched unique microbial taxa within the microbiota of TC origin, including *RG*. This *RG*-enriched microbiota induced lupus-like autoimmune responses and gut inflammation in nonautoimmune B6 mice. Furthermore, Trp promoted the in vitro growth of the LG-producing *RG* strain, which metabolized Trp differently than a control-type strain. Overall, these results suggest a model of pathogenesis in which genetic susceptibility drives the development of an inflammatory immune system that shapes the microbiome toward an altered Trp catabolism. This in turn favors the gut expansion of *RG*, which may promote autoimmune responses.

MATERIAL AND METHODS

Mice and treatment. TC, TC.*Rag*1$^{-/-}$ mice, which have been described previously,[8,12] and B6 mice were maintained at the University of Florida or University of Texas Health Science Center at San Antonio in specific pathogen-free (SPF) conditions. Mice were housed within the same strain and the same age group. Unless specified, mice were fed with irradiated Envigo 7912 standard chow. Only female mice were used, corresponding to the accelerated disease development in the TC model.[8] For colonization with the LG-producing strain (CC55_001C NIH, *RG2*) and the nonproducing strain (29149 ATCC, *RG1*), two-month-old TC and B6 preconditioned mice with a cocktail of antibiotics (ampicillin and metronidazole [0.05%; Fisher], neomycin [0.05%; Cayman], and vancomycin [0.025 %; Cayman] [AMNV]) in the drinking water for two weeks, were gavaged with 10^8 colony forming unit (CFU) of bacteria daily for five days, two days after AMNV was discontinued. Controls were age-matched, AMNV-conditioned mice. A second cohort of TC AMNV-preconditioned mice were gavaged with *RG2* for seven consecutive days before they were killed. To deplete *RG* during development, two-month-old TC mice were treated with 0.15 % metronidazole in drinking water for five to seven months, and *RG* depletion was tested after one month of treatment in fecal samples by quantitative polymerase chain reaction (qPCR).

FMT was performed as previously described,[13] with feces from TC donors displaying high serum anti–double-stranded DNA (anti-dsDNA) IgG titers, and from sex- and age-matched B6 mice into eight-week-old B6 recipients that were either germ-free (GF) or AMNV-preconditioned mice. Recipients were fed with high (1.19%) or low (~0.03%) Trp chow (Research Diets) as previously described[9] for one week before FMT and continued for three weeks after FMT. Gut permeability was evaluated with fluorescein isothiocyanate (FITC)–dextran 4000 (Sigma-Aldrich), as previously described.[14] The effect of Trp restriction on fecal *RG* levels was compared longitudinally in TC mice switched from standard to a low Trp diet at two months of age for up to 28 weeks to age-matched controls on a Trp control (0.8%) chow. All animal protocols were approved by the Institutional Animal Care and Use Committee from each institution.

Bacterial assays and ex vivo exposure to immune cells. Fecal DNA was extracted with a DNeasy PowerLyzer PowerSoil Kit (Qiagen). Total bacterial DNA and *RG* abundance were measured by qPCR with 16S ribosomal DNA (rDNA) primers (Table S1). *RG* abundance was presented as a percentage of 100 ng total fecal DNA used for each reaction. Individual *RG1* and *RG2* colonies streaked on Tryptic Soy Agar blood plates (Fisher) were grown in brain heart infusion media (Anaerobe Systems) under anaerobic conditions for 16 hours. CFUs were calculated from OD600 readings based on growth curves. Bacterial growth was evaluated in response to supplemental Trp, either as OD600 at four hours with 100 μ*M* Trp, or CFU at six hours with 2 m*M* Trp. Metabolites were compared between *RG1* and *RG2* cultured with or without 2 m*M* Trp for four hours. Mesenteric lymph node (mLN)

cells (2×10^5) were exposed to lysates prepared from sonicated bacteria at 1:10 mLN cell:bacteria ratio and stimulated with 1 μg/mL anti-CD3 and anti-CD28 antibodies (BD Biosciences) in complete RPMI medium (Corning). After 72 hours, $CD4^+$ T cell phenotypes were evaluated by flow cytometry. In some assays, bone marrow–derived dendritic cells (BMDCs), generated as previously described,[15] were cocultured with B6 Treg cells in the presence of bacterial lysates at a 1:1:10 BMDC:Treg:bacteria ratio or 100 ng/mL lipopolysaccharide (LPS). Purified Treg cells were cultured with lysates at a 1:1 CFU ratio. Apoptosis was evaluated by flow cytometry after 48 hours. Cytokines were quantified in the supernatant of BMDCs stimulated with bacterial lysates at a ratio of one cell:bacterial CFU for 48 hours with the Luminex multiplex cytokine kit (Biorad).

Histology. Frozen sections were prepared as previously described.[14] Kidney sections were stained with anti-CD3e-APC (eBioscience 145-2C11). Ileum sections were stained with rabbit anti-Claudin-1 (Invitrogen MH25), followed by goat anti-rabbit IgG-AF700 (Invitrogen A-21038). Colon sections were stained with anti-CD45-APC/Cyanine7 (Biolegend 30-F11) and anti-IgA-FITC (BD Biosciences). Fluorescence intensity was analyzed using ImageJ.

Antibody and cytokine measurements. Serum and fecal anti-dsDNA antibodies were quantified by enzyme-linked immunosorbent assay (ELISA) with 1:100 dilutions, as previously described.[9] Anti-dsDNA IgG was also visualized on *Crithidia luciliae* slides (Biorad) in serum diluted 1:10, followed by incubation with goat anti-mouse IgG-FITC (Southern Biotech). The fluorescence from each *Crithidia luciliae* cell was quantified with ImageJ. Interleukin-6 (IL-6) or interferon-γ (IFN-γ) levels were quantitated with BD Biosciences ELISA kits in serum diluted 1:50 in duplicate.

Flow cytometry. Single-cell suspensions were isolated from the gut using the lamina propria dissociation kit with gentleMACS tissue dissociator (Miltenyi Biotech) or from the spleen and mLN, as previously described.[16] Fluorochrome-conjugated antibodies used in this study are listed in Table S2. Samples were acquired on an LSR Fortessa flow cytometer (BD Biosciences) and analyzed with FlowJo software. Gating strategies are shown in Supplemental Figures 1 and 2.

16S rDNA amplicon sequencing. Libraries were constructed and sequenced as described previously.[17] Briefly, 2 × 300–bp paired-end reads per sample with a minimal sequence depth of 44,966 were obtained. Using QIIME 2 (version 2020.8), reads were merged, quality trimmed, and clustered into operational taxonomic units at 97% sequence similarity. Taxonomy was assigned using Greengenes 13_8.

Metabolomic analysis. Cultured bacteria were processed for metabolomic analysis as described previously.[17] All samples were normalized by total protein content before extraction and run in both positive and negative ionization modes on a Thermo Q-Exactive Orbitrap mass spectrometer. Metabolic pathway analysis was performed using *Mummichog*.[18] Pathways represented by at least two significant metabolites in positive or negative mode are presented. Additional metabolites, indicated with asterisks in heatmaps, were annotated based on their enrichment in significant pathways and by the m/z match with an accuracy of 10 parts per million.

Statistics and data availability. Statistical analyses were performed with the GraphPad Prism 9.0 software with two-tailed tests, as indicated in the figure legends. The 16S rDNA amplicon sequencing and bacteria metabolomic data sets are available on request directly to the corresponding author.

RESULTS

***RG* promoting autoimmune activation in TC mice.** We evaluated the role of *RG* strains in autoimmune activation by colonizing antibiotic-pretreated TC mice with LG-producing *RG2* bacteria compared to aged-matched controls (Figure 1A). One week after colonization with *RG2*, TC mice displayed a reduced frequency of splenic $CD25^{high}$ Treg cells that presented a reduced CD25 expression, and total Treg cells in the colon with an increased FoxP3 expression (Figure 1B–E). These results suggest that *RG2* alters Treg populations early after exposure. One month after colonization, *RG2* remained detectable in TC fecal samples but returned to baseline levels after two months (Figure 1F and G). Comparatively, the abundance of non–LG-producing *RG1* was much lower (Supplemental Figure 3A). In addition, *RG2* gavage of three independent B6 cohorts failed to produce detectable levels of RG2 at the same time point (Supplemental Figure 3B). In TC mice, *RG2* colonization increased levels of serum anti-dsDNA IgG (Figure 1H) and induced the production of anti-LG IgG, in direct correlation with anti-dsDNA IgG (Figure 1I and J). This reiterated the same correlation of anti-LG with anti-dsDNA IgG serum levels reported in patients with SLE.[4] *RG2* also increased the frequency of splenic activated $CD69^+CD4^+$ T cells, effector memory $CD4^+$ T cells, as well as IFN-γ producing $CD4^+$ T cells and IL-10–producing nonregulatory T cells, two cell types expanded in patients with SLE,[19,20] with a concurrent decrease in the frequency of naïve $CD4^+$ T cells (Figure 1K–O). Additionally, *RG2* increased the frequency of germinal center B cells in the spleen (Figure 1P).

To further test the role of *RG* in the development of autoimmunity, we treated two-month-old TC mice with metronidazole, which kills most, although not all, anaerobes.[21] Fecal *RG* was depleted without affecting the total bacterial content (Figure 2A and B). After five or seven months of treatment, *RG* depletion

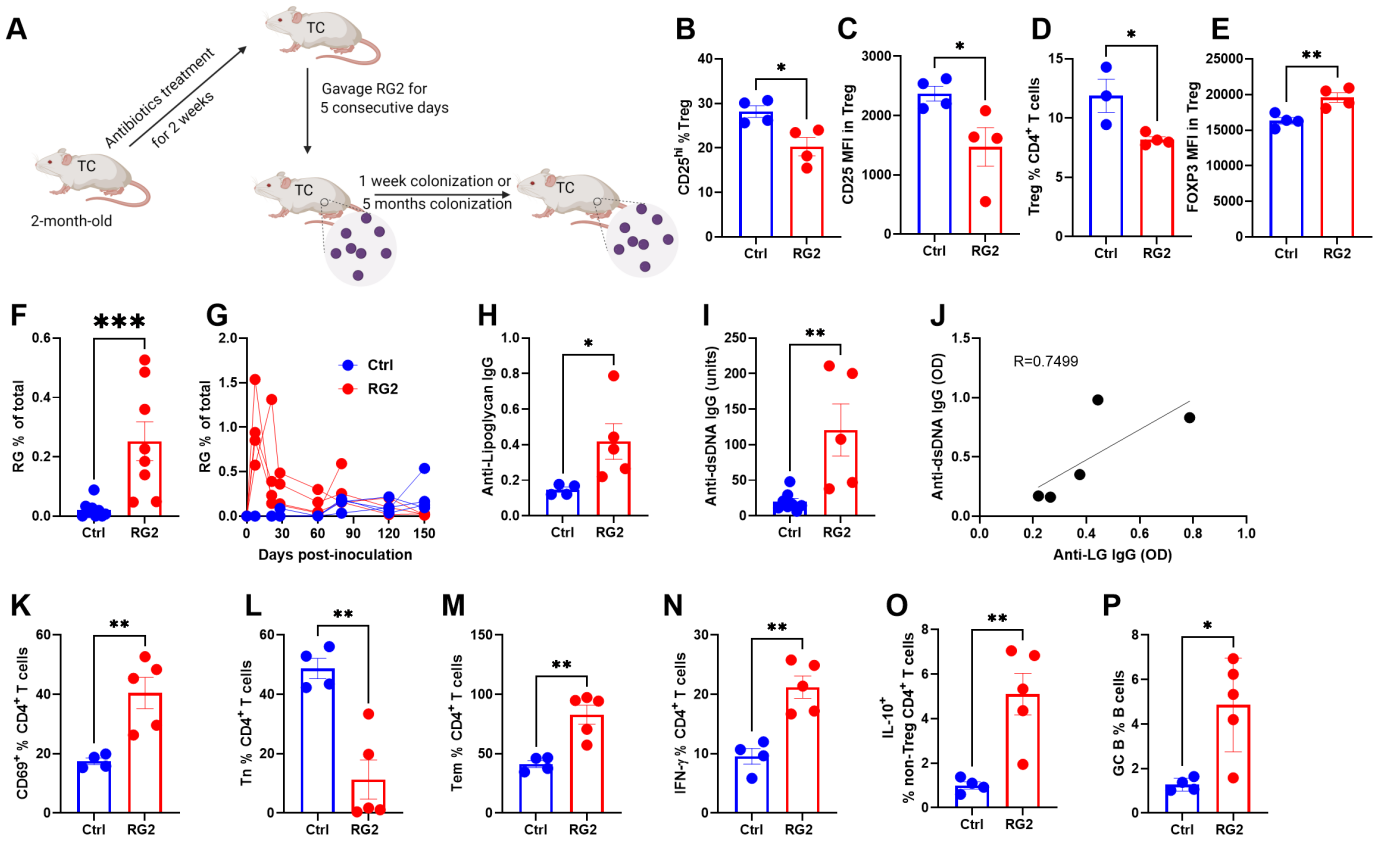

Figure 1. *RG2* promoted autoimmune activation in TC mice. (A) Experimental design with recipients analyzed (B–E) one week or (F–P) five months after *RG2* colonization. Ctrls were age-matched mice conditioned with the antibiotic treatment but not colonized with any bacteria. Frequency of splenic $CD25^{high}$ (B) Treg cells and (C) their CD25 mean fluorescence intensity (MFI). (D) Treg cells in the colon with (E) FoxP3 MFI. (F) *RG* levels in Ctrl and *RG2*-colonized TC mice 28 days after inoculation (stool samples pooled from two cohorts). (G) Longitudinal fecal RG levels after *RG2*-colonization in individual TC mice and controls. Serum (H) anti-LG and (I) anti-dsDNA IgG and (J) correlation between the two. Frequency of (K) splenic $CD69^+CD4^+$ T cells, (L) naïve $CD4^+$ T cells, (M) effector memory $CD4^+$ T cells, (N) IFN-γ^+CD4^+ T cells, (O) IL-10–producing non-Treg $CD4^+$ T cells, and (P) germinal center B cells. Mean + SEM compared with *t*-tests. $^*P < 0.05$; $^{**}P < 0.01$. anti-dsDNA, anti–double-stranded DNA; anti-LG, anti-lipoglycan; Ctrl, control; IFN-γ, interferon-γ; IL-10, interleukin-10; OD, optical density; RG, *Ruminococcus gnavus*; TC, B6.*Sle1*.*Sle2*.*Sle3* triple congenic.

was associated with reduced markers of disease activity in lupus such as anti-dsDNA IgG levels, splenomegaly, $CD4^+$ T cell expansion, and the ratio of follicular T helper to follicular Treg (Tfr) cells, associated with a relative expansion of Tfr cells (Figure 2C–F; Supplemental Figure 4A and B). On the other hand, *RG* depletion was associated with increased CD25 and FoxP3 expression by Treg cells (Figure 2G–I). In patients with SLE, Treg cells expressing low levels of CD25 and FoxP3 have a reduced suppressive function and are expanded.[22] The frequency of Treg cells was also increased in the mLN of these treated mice (Figure 2J), suggesting an expansion at sites closer to the gut microbiota. Taken together, our results suggest that *RG2* expansion, which occurs preferentially in gavaged TC mice, induced autoimmune activation, whereas *RG* depletion correlated with expansion of Treg cell populations in these mice.

To directly investigate the impact of *RG2* on $CD4^+$ T cells, mLN cells from untreated B6 and TC mice were stimulated with anti-CD3/CD28 antibodies in the presence of *RG1* or *RG2* lysates, relative to the medium alone. Either *RG1* or *RG2* reduced the frequency of both B6 and TC Treg cells (Figure 2K), and there was no effect on Treg cell proliferation (Figure 2L). However, when stimulated in the presence of *RG2*, a higher level of activated caspase 3 was detected in Treg cells but not in non-Treg $CD4^+$ T cells (Figure 2M, Supplemental Figure 4C). Both *RG1* and *RG2* lysates enhanced the apoptosis of Treg cells cocultured with BMDCs as compared to control bacteria or LPS (Figure 2N). However, direct exposure to bacterial lysate failed to induce apoptosis in purified Treg cells (Supplemental Figure 2D), suggesting the involvement of DCs in the induction of Treg apoptosis. Further, BMDCs stimulated with *RG1* produced high levels of both IL-10 and tumor necrosis factor α (TNF-α), whereas *RG2* only induced the production of modest amounts of TNF-α (Figure 2O and P). Taken together, these results suggest that *RG2* may reduce the

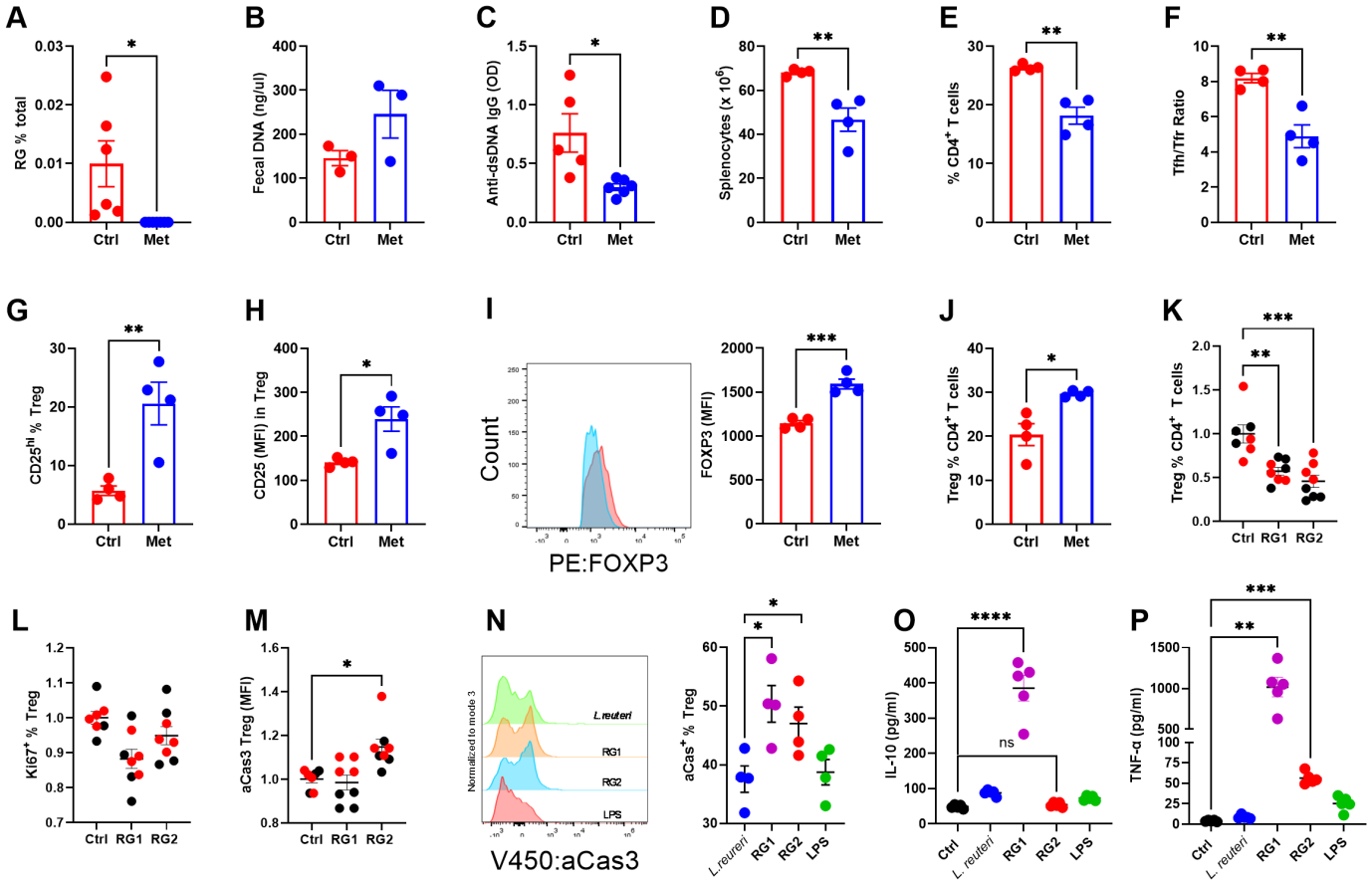

Figure 2. *RG* depletion is associated with a reduction in autoimmune activation in TC mice. (A) Fecal *RG* and (B) total microbial DNA levels in control and Met TC mice one month into treatment. Immune phenotypes were assessed five to seven months into treatment. (C) Serum anti-dsDNA IgG. (D–I) Splenocytes: (D) cell counts, (E) frequency of $CD4^+$ T cells, (F) Tfh:Tfr cell ratio, (G) frequency of $CD25^{high}$ Treg cells, (H) CD25, and (I) FoxP3 expression by Treg cells, with representative FoxP3 FACS plots. (J) Treg cell frequency in mLN $CD4^+$ T cells. (K–N) B6 (black) and TC (red) mLN cells were stimulated with anti-CD3/CD28 antibodies in the presence of *RG1* or *RG2* lysate for 72 hours. Ctrl cells were stimulated without bacterial lysates. Frequency of (K) Treg and (L) $Ki67^+$ Treg cells. (M) Activated caspase 3 levels in Treg cells normalized to the mean values for controls set as 1. (N) Frequency of activated caspase 3 positive cells in Treg cells cocultured with bone marrow–derived dendritic cells (BMDCs) and different bacterial lysates with representative overlay histograms shown on the left. (O) IL-10 and (P) TNF-α levels produced by BMDCs stimulated with bacterial lysates compared to unstimulated controls. (A–J) *t*-tests, (K–P) one-way analysis of variance with multiple-comparisons tests. $^*P < 0.05$; $^{**}P < 0.01$; $^{***}P < 0.001$. anti-dsDNA, anti–double-stranded DNA; B6, C57BL/6; Ctrl, control; IL-10, interleukin-10; Met, metronidazole treated; mLN, mesenteric lymph node; RG, *Ruminococcus gnavus*; TC, B6.*Sle1.Sle2.Sle3* triple congenic; Tfh, follicular T helper; Tfr, follicular Treg; TNF-α, tumor necrosis factor α.

frequency of Treg cells by inducing their apoptosis, which may be partially mediated by a cytokine imbalance in DCs.

Fecal communities of lupus-prone TC mice naturally enriched in *RG*. Because *RG* blooms correspond to disease flares in patients with SLE,[5] we tested the hypothesis that *RG* populations may expand during disease progression in TC mice. We longitudinally measured total fecal *RG* abundance, as 16S rDNA amplicons cannot distinguish *RG2* from *RG1*,[5] in two cohorts of age-matched TC and B6 mice housed in separate buildings. TC and B6 mice had similarly low *RG* levels in the first three months of age (Figure 3A), when TC mice do not produce autoantibodies yet. Later, the *RG* population significantly expanded in TC mice, while remaining relatively lower in B6 mice. Interestingly, a much lower *RG* level was detected in TC.$Rag1^{-/-}$ mice, which lack mature T and B cells (Figure 3B), suggesting that adaptive immunity is necessary for the expansion of *RG* in lupus-prone mice. Serum anti-dsDNA IgA and IgM levels were significantly higher in TC mice with an *RG* abundance above the median (Table S3), and a similar trend was observed for anti-dsDNA IgG (Figure 3C–E). Serum IL-6 and IFN-γ, two inflammatory cytokines that are overexpressed in patients with SLE,[19,23] were also positively correlated with *RG* abundance in these mice (Figure 3F and G). These results suggest that *RG* expands in TC mice as they start producing autoantibodies in correlation with markers of inflammation.

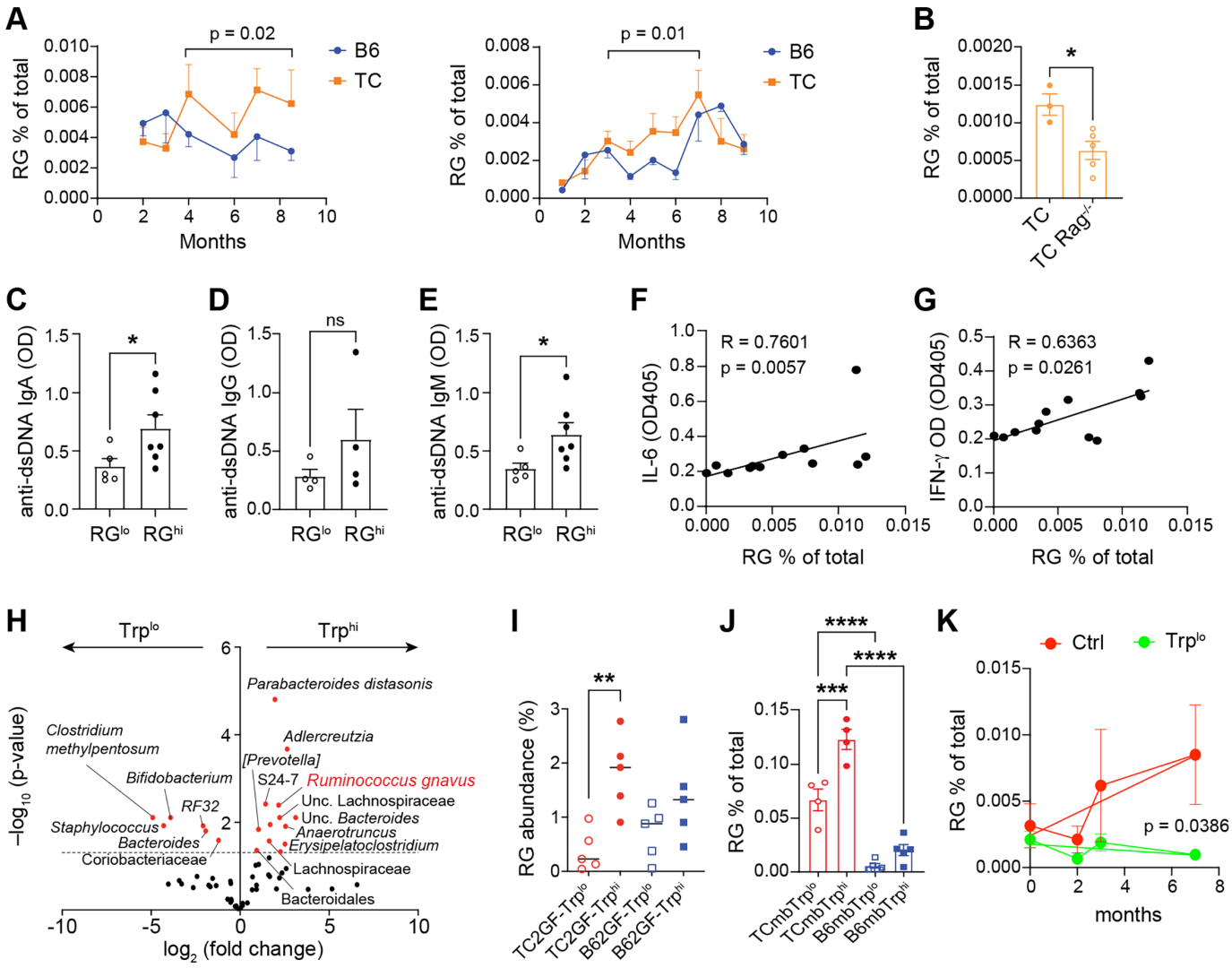

Figure 3. Dietary tryptophan expanded *RG* abundance in TC microbiota. (A) Longitudinal fecal *RG* abundance in two cohorts of TC and B6 mice (n = 4–5 per group). Brackets indicate significant differences by two-way analysis of variance (ANOVA). (B) Fecal *RG* levels in three-month-old TC and TC.Rag1$^{-/-}$ mice. (C–G) Six- to nine-month-old TC mice were assessed for fecal *RG* levels and (C) serum anti-dsDNA IgA, (D) anti-dsDNA IgG, (E) anti-dsDNA IgM, (F) IL-6, and (G) IFN-γ. In D–E, mice were distributed in *RG*^{low} and *RG*^{high} groups relative to the median level and compared with Mann-Whitney tests. IL-6 correlation was evaluated with a Spearman and IFN-γ with a Pearson test. (H) Volcano plot showing taxa differentially enriched by tryptophan in B6 mice receiving fecal microbiota transfer (FMT) from TC microbiota. *RG* relative abundance in the four groups of FMT recipients measured by (I) 16S rDNA sequencing and (J) qPCR was compared with one-way ANOVA with multiple-comparisons tests. (K) *RG* fecal levels in TC mice on Trp^{low} or control diets started at 8 weeks of age for 28 weeks (n = 6 per group) compared with a two-way ANOVA. Simple linear regression lines are shown for each group. Mean + SEM, $^{*}P < 0.05$; $^{**}P < 0.01$; $^{***}P < 0.001$; $^{****}P < 0.0001$. anti-dsDNA, anti–double-stranded DNA; B6, C57BL/6; IL-6, interleukin-6; IFN-γ, interferon-γ; qPCR, quantitative polymerase chain reaction; rDNA, ribosomal DNA; RG, *Ruminococcus gnavus*; TC, B6.*Sle1.Sle2.Sle3* triple congenic; Trp, tryptophan.

Trp expanding *RG* abundance in the TC microbiota. We have shown that dietary Trp alters the gut microbiota differently in lupus-prone and healthy control mice.[9,10] Here, we evaluated the impact of dietary Trp on gut microbiota without the confounding effect of lupus-susceptibility genes on immune activation or intrinsic Trp metabolism. In these studies, we performed FMTs from TC or B6 donors into GF B6 recipients fed with a high or low Trp diet. This resulted in four groups of recipient mice: TC microbiota fed high Trp (TCmbTrp^{high}) or TC microbiota fed low Trp (TCmbTrp^{low}) and B6 microbiota fed high Trp (B6mbTrp^{high}) or B6 microbiota fed low Trp (B6mbTrp^{low}) (Supplemental Figure 5A). Principal component analysis showed distinct microbiota profiles for the TCmbTrp^{high} and B6mbTrp^{low} groups, with an overlap between the TCmbTrp^{low} and B6mbTrp^{high} groups (Supplemental Figure 5B). The Trp^{high} diet resulted in either the enrichment or depletion of several bacterial species in microbiota communities of either TC or B6 origin (Figure 3H; Supplemental Figure 5C–E). However, high Trp also enriched specific taxa

depending on the origin of the microbiota (Figure 3H; Supplemental Figure 5F–M).

Noticeably, the TCmbTrp^{high} samples contained the highest number of taxa with a significantly different abundance, 7 of 10 of which were uniquely enriched in TCmbTrp^{high} recipients, including increased representation of *RG* (Figure 3H and I), which was confirmed by qPCR analysis in an independent cohort of FMT recipients (Figure 3J). The qPCR analysis also showed the respective influences of the microbiota origin and dietary Trp, with *RG* abundance being higher in TCmbTrp^{low} than in B6mbTrp^{high} mice, with a similar trend between B6mbTrp^{high} and B6mbTrp^{low} mice. These results suggest that both dietary Trp and the host origin of the microbiota, which itself is highly determined by genetics, shaped the architecture of the gut microbiota community, including *RG* abundance. Finally, a low Trp diet started at two months of age prevented the progressive endogenous *RG* expansion in TC mice (Figure 3K), suggesting that the beneficial effects of low Trp in TC mice[9] may be partially driven by limiting *RG* abundance.

Microbiota from lupus-prone mice combined with high dietary Trp in promoting autoimmune activation and intestinal inflammation. Levels of anti-dsDNA IgA as well as serum total IgA were higher in TCmbTrp^{high} mice than either B6mbTrp^{high} or B6mbTrp^{low} mice, with intermediate values in TCmbTrp^{low} mice (Figure 4A and B), and TCmbTrp^{high} mice were the only group to produce high levels of anti-dsDNA IgA detected in the cecum (Figure 4C). Cecal total IgA was also most

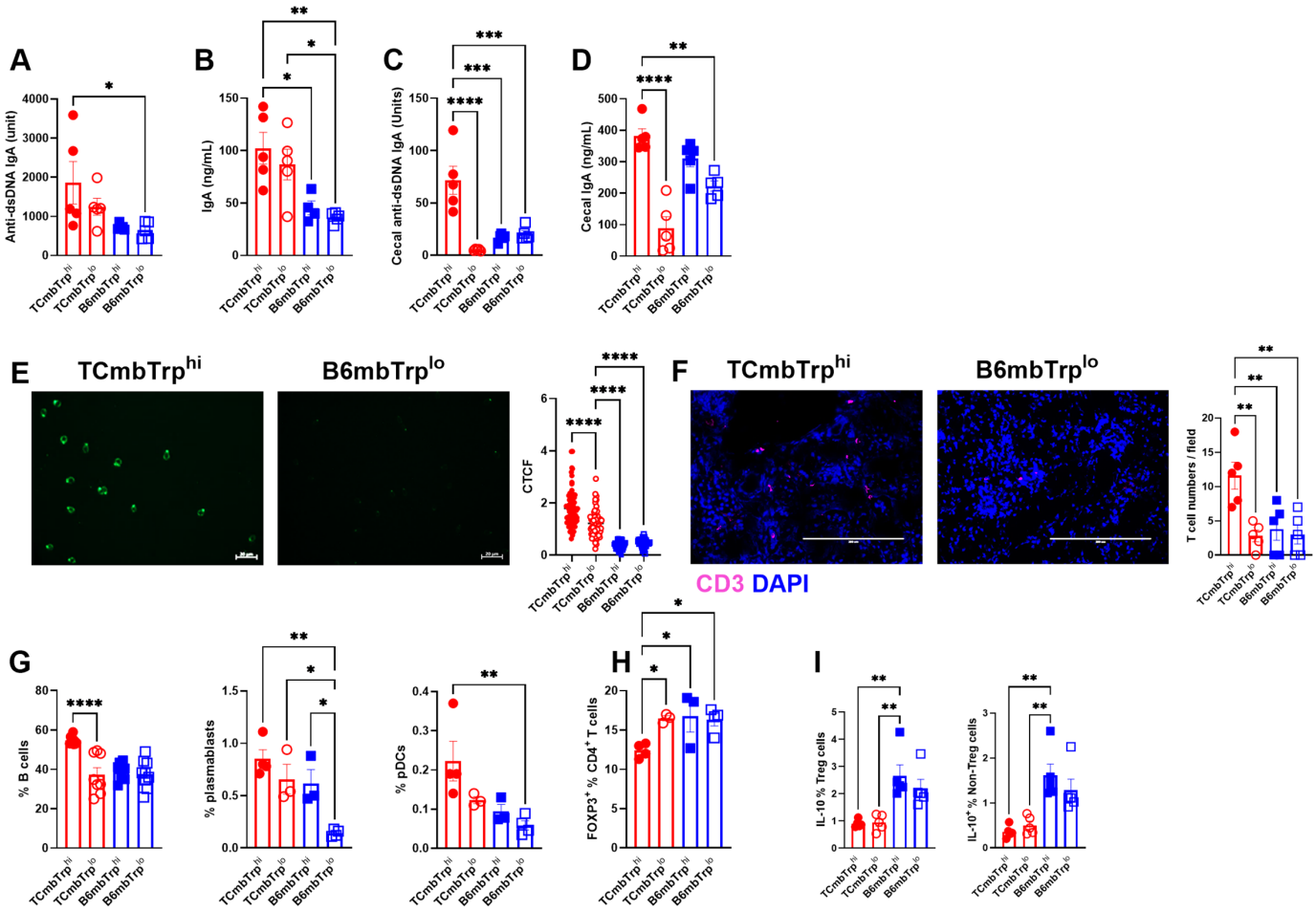

Figure 4. The combination of gut microbiota from lupus-prone mice and high dietary tryptophan promoted autoimmune activation. (A) Terminal serum anti-dsDNA IgA and (B) total IgA. (C) Terminal cecal anti-dsDNA IgA and (D) total IgA. (E) Representative images (scale bar: 20 μm) and quantitation of *Crithidia luciliae* assays on terminal serum. CTCF calculated on all visible IgG$^+$ cells. n = 3 to 9 FMT recipients per group. (F) Representative images (scale bar: 200 μm) and quantitation of CD3$^+$ cell infiltrates in the kidney. All CD3$^+$ cells were counted in the ×20 field. (G) Frequency of splenic B cells, plasmablasts, and pDCs. Frequency of mLN Treg cells in (H) CD4$^+$ T cells and (I) IL-10$^+$ cells in Treg and non-Treg CD4$^+$ T cells. Mean + SEM compared with one-way analysis of variance with multiple-comparison tests. *P < 0.05; **P < 0.01; ***P < 0.001; ****P < 0.001. anti-dsDNA, anti–double-stranded DNA; B6mbTrp, C57BL/6 microbiota fed tryptophan; CTCF, corrected total cell fluorescence; DAPI, 4',6-diamidino-2-phenylindole; IL-10, interleukin-10; mLN, mesenteric lymph node; pDC, plasmacytoid dendritic cell; TCmbTrp, B6.*Sle1.Sle2.Sle3* triple congenic microbiota fed tryptophan.

abundant in TCmbTrp^{high} mice (Figure 4D). The dsDNA-specific *Crithidia luciliae* indirect immunofluorescence assay detected a higher level of anti-dsDNA IgG in the serum of TCmbTrp^{high} mice compared to all the other groups (Figure 4E). In addition, the serum anti-dsDNA IgA:IgM ratio was higher in TCmbTrp^{high} mice than in the three other groups, and there was a similar trend for the anti-dsDNA IgG:IgM ratio (Supplemental Figure 6A and B). Because these ratios have been correlated with LN[24] and T cells are a major contributor to end-organ damage, we assessed T cell infiltration in the kidneys of FMT recipients. Consistent with these findings, a higher level of CD3$^+$ T cell infiltration was detected in the TCmbTrp^{high} kidneys than in the three other groups (Figure 4F). These findings support the notion that Trp-mediated microbiota changes accelerate LN in TC mice.

A higher frequency of B cells, plasmablasts, and plasmacytoid DCs, three immune cell types involved in SLE, were found in

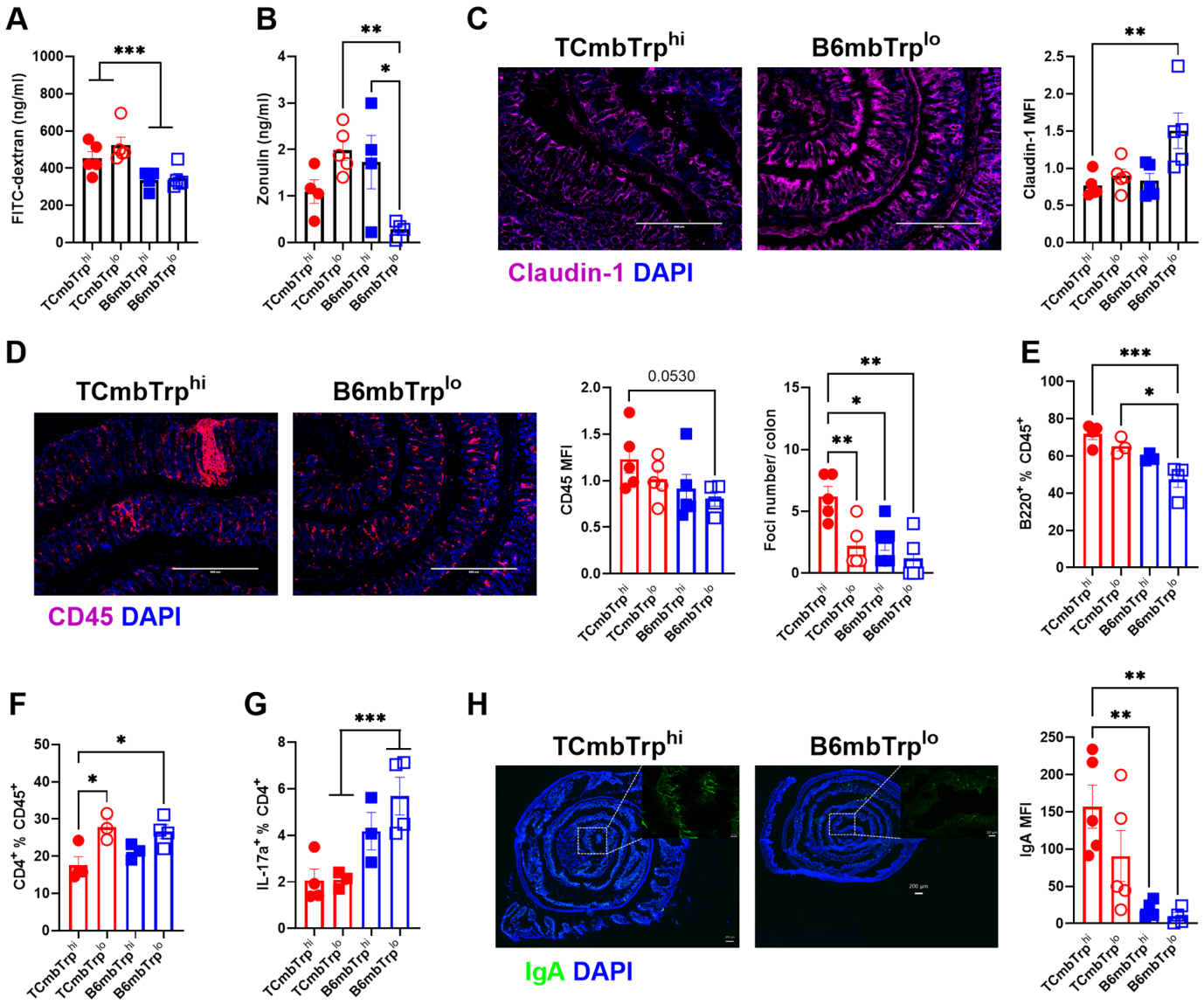

Figure 5. Gut microbiota from lupus-prone mice and high dietary Trp promote intestinal inflammation. (A) Serum FITC-dextran concentration after FITC-dextran gavage. (B) Serum zonulin concentration. Representative images (scale bars: 400 μm) of TCmbTrp^{high} and B6mbTrp^{low} ileums stained for (C) Claudin-1 and (D) colons stained for CD45 with MFI quantitation shown on the right, along with the number of CD45$^+$ foci. (E–H) Flow cytometry analysis of the colon lamina propria. Frequency of (E) B220$^+$ B cell, (F) CD4$^+$ T cells among CD45$^+$ cells, and (G) IL-17a$^+$ CD4$^+$ T cells. (H) Representative images (scale bars: 200 μm) of colon stained for IgA with IgA MFI on the right. Mean + SEM compared with one-way analysis of variance with multiple-comparison tests (B–F and H), or *t*-tests between grouped samples according to the origin of the microbiota (A and G). *P < 0.05; **P < 0.01; ***P < 0.001; ****P < 0.0001. B6mbTrp^{low}, C57BL/6 microbiota fed high tryptophan; DAPI, 4',6-diamidino-2-phenylindole; FITC, fluorescein isothiocyanate; IL-17a, interleukin 17a; MFI, mean fluorescence intensity; TCmbTrp^{high}, B6. *Sle1.Sle2.Sle3* triple congenic microbiota fed high tryptophan; Trp, tryptophan.

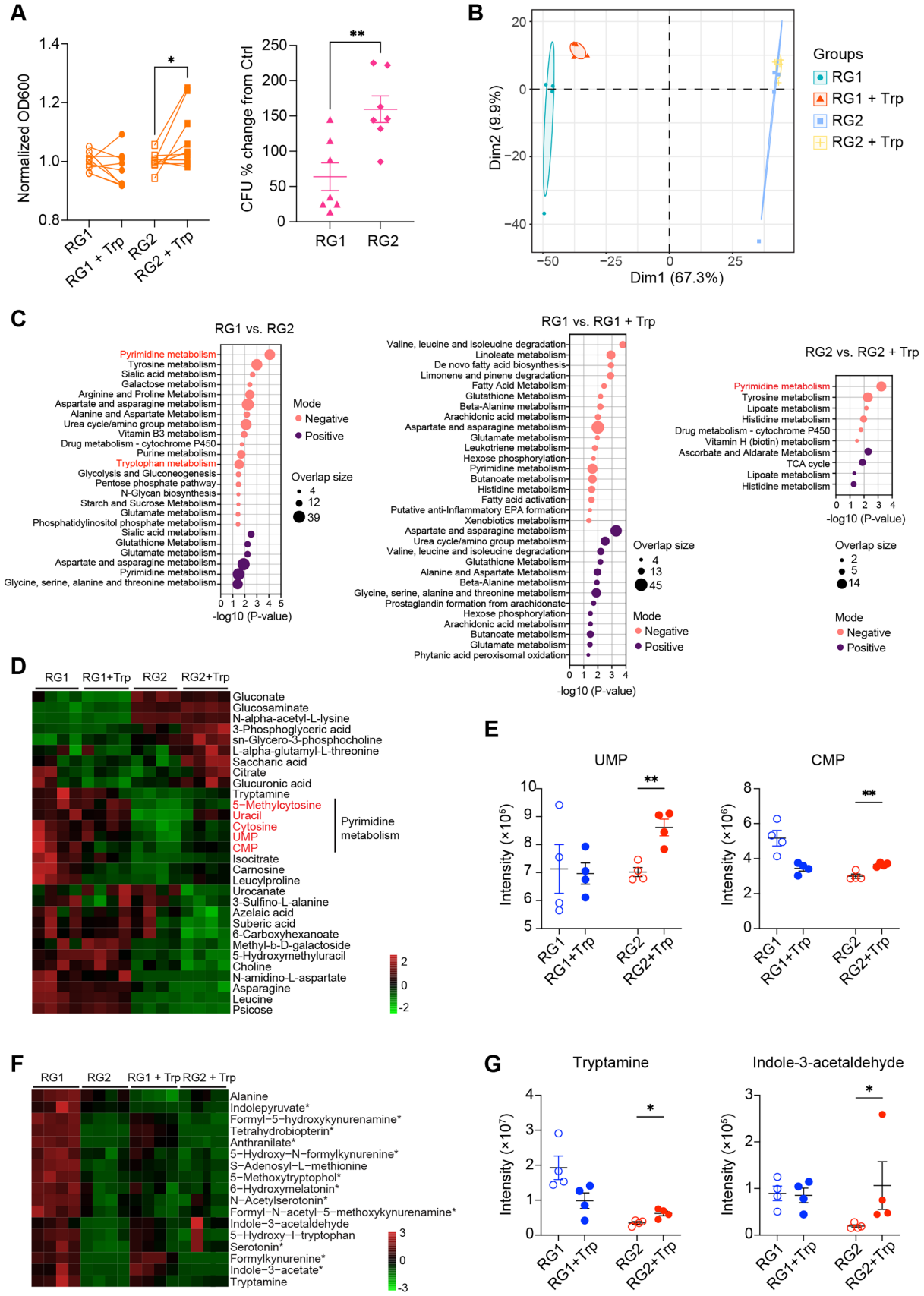

Figure 6. Legend on next page.

TCmbTrp^{high} spleens (Figure 4G). Although the distribution of the major splenic CD4$^+$ T cell effector subsets was similar among the four recipient groups, a lower frequency of FoxP3$^+$ Treg cells was observed in the mLN of TCmbTrp^{high} mice (Figure 4H). Furthermore, the frequency of IL-10–producing Treg and non-Treg CD4$^+$ T cells were also lower in the mLN of mice that received TC microbiota, regardless of Trp (Figure 4I). Overall, these results suggest that high dietary Trp altered the composition of the gut microbiota originating from autoimmune TC mice, including *RG* expansion, which promoted inflammatory pathogenesis even in mice with a nonautoimmune genetic background.

Because *RG2* colonization impaired intestinal barrier functional integrity in GF B6 mice in a zonulin-mediated process,[6] we investigated the effects of the FMT combined with dietary Trp on the intestinal environment of B6 recipients. The transfer of TC microbiota increased gut permeability in B6 mice regardless of dietary Trp (Figure 5A). The lowest level of serum zonulin, a marker of functional barrier integrity,[25] and the highest expression of the tight junction protein, Claudin-1, occurred in the ileum of B6mbTrp^{low} mice (Figure 5B and C), suggesting that both the TC microbiota and high dietary Trp disrupt intestinal barrier integrity. Additionally, TCmbTrp^{high} mice developed the highest number of CD45$^+$ leukocytes and immune foci in the colon (Figure 5D). Colons of B6mbTrp^{low} mice showed the lowest frequency of B cells (Figure 5E), whereas the Trp^{low} diet increased the frequency of CD4$^+$ T cells regardless of the origin of the microbiota (Figure 5F). Recipients of TC microbiota displayed a lower frequency of IL-17A$^+$CD4$^+$ T cells, regardless of Trp (Figure 5G), consistent with an impaired gut barrier because IL-17A$^+$ T cells may play a protective role.[26] Finally, a large number of IgA$^+$ cells were detected in the colon of TC microbiota recipients that was enhanced by dietary Trp (Figure 5H), consistent with the high production of IgA and anti-dsDNA IgA. Taken together, TC-derived microbiota drives gut inflammation and alters barrier integrity, which is modulated by dietary Trp.

Trp promoting growth of LG-producing *RG* strain. The growth of LG-producing *RG2*, but not *RG1*, was enhanced by Trp in vitro (Figure 6A). Following culture in a standard medium, untargeted bacterial metabolomics analyses showed global differences between the *RG1* and *RG2* profiles, which were further enhanced by supplemental Trp, albeit to a lesser extent for *RG2* (Figure 6B). Pyrimidine metabolism was the top pathway differing between the two strains at baseline and between baseline and supplemental Trp for *RG2*, whereas amino acid and fatty acid metabolism were the major pathways impacted by Trp in *RG1* (Figure 6C). Five metabolites in the pyrimidine pathway, including UMP and CMP, were uniquely enriched by Trp in *RG2* (Figure 6D and E). These observations suggest that Trp promoted pyrimidine biosynthesis, which may contribute to *RG2* expansion. Trp metabolism also differed between *RG1* and *RG2* (Figure 6C–F). In standard medium, *RG2* produced less tryptamine and indole-3-acetaldehyde (IAAld) than *RG1*, whereas supplemental Trp increased their production only in *RG2* (Figure 6G). These observations suggest that *RG2* possesses a differential Trp catabolic pathway that correlates with pathogenic potential.

DISCUSSION

RG is a gut pathobiont that is expanded in patients with SLE in direct correlation with disease activity, and *RG* strains isolated from patients with SLE produce a proinflammatory highly immunogenic novel lipoglycan.[4,5] *RG* strains have been reported in the feces of healthy B6 mice.[27] Here, we showed that *RG* is represented within the microbiome of lupus-prone TC mice with a higher abundance than in the healthy congenic B6 controls, and that its depletion along with that of most anaerobes is associated with a reduction of autoimmune activation. Gavaged LG-producing *RG* strain, *RG2*, persistently colonized TC but not congenic B6 mice. *RG2* colonized GF B6 mice by vertical transmission,[6] and the difference in outcomes with the current study may be due to the continuous postnatal exposure to parental *RG2*, or a greater ability for *RG2* to colonize neonates relative to adult mice. Nonetheless, these results suggest that LG-producing *RG* is preferentially expanded in genetically predisposed TC mice as compared to healthy controls, which may correspond to the intestinal blooms observed in patients with SLE with high disease activity.[4,5] Although the non-LG-producing strain *RG1* colonized GF B6 mice,[6] it was not able to colonize either TC or B6 mice in SPF condition, suggesting that it has a reduced capacity to compete with other commensals as compared to *RG2*.

Figure 6. Differential effect of tryptophan on putative pathobiont *RG2* and its control strain *RG1*. (A) In vitro *RG1* and *RG2* growth measured as OD600 with or without 100 μ*M* L of Trp four hours after inoculation, and as CFU changes induced by 2 m*M* L of Trp six hours after inoculation. (B) PCA plots of metabolite features among *RG*1, *RG2*, *RG1*+Trp, and *RG2*+Trp. (C) Pathway analysis of metabolites with significantly differing intensity between *RG1* and *RG2*, between *RG1* and *RG1*+Trp, and between *RG2* and *RG2*+Trp. (D) Heatmap of metabolites showing significantly different intensity between *RG2* and *RG2*+Trp, but not between *RG1* and *RG1*+Trp. Pyrimidine metabolites are highlighted in red font. (E) Abundance of UMP and CMP in the four groups. (F) Heatmap of signature tryptophan metabolites (indicated by a star) among the four groups. (G) Abundance of tryptamine and indole-3-acetaldehyde in the four groups. Mean + SEM compared with paired *t*-tests (A, left graph) and unpaired *t*-tests (A, right graph, E, and G). *$P < 0.05$; **$P < 0.01$. CFU, colony forming unit; Ctrl, control; PCA, principal components analysis; RG, *Ruminococcus gnavus*; Trp, tryptophan.

Colonization with *RG2* accelerated inflammatory autoimmune pathogenesis, including the production of autoantibodies in TC mice, which confirmed the results obtained in GF mice colonized with LG-producing *RG* strains.[6] *RG2* also induced early activation of T cells in the colon and the spleen of TC mice. Conversely, the depletion of metronidazole-sensitive anaerobes, which included *RG*, decreased autoimmune activation and increased the frequency of Treg cells with a higher CD25 and FoxP3 expression. We showed that *RG2* lysates induced Treg cell apoptosis, but not directly. The control *RG1* strain also induced Treg cell apoptosis by altering DC functions, but its inability to colonize mice makes it nonpathogenic. In addition, *RG1* but not *RG2* induced a large amount of IL-10 by DCs, and IL-10 plays a critical role in maintaining Trg cell integrity.[28–30] In addition, B6 and TC Treg cells were equally affected by *RG2*, but B6 mice are resistant to persistent *RG2* expansion, and therefore their Treg cells could not be targeted in vivo. These results suggest that *RG2*, which has a unique ability for long-term colonization of lupus-prone mice, plays a direct role in autoimmune activation, at least partially by targeting Treg cells. The changes in autoimmune activation associated with *RG* levels could also be indirect through the alterations in the microbiome induced by the expansion or the reduction of RG abundance. *Ruminococcus* abundance has been positively correlated with the number of Treg cells in patients with SLE.[31] However, this result should be interpreted with caution because *RG* has been reclassified out of the *Ruminococcus* family.[7]

RG has recently been shown to be expanded in mice by the combination of triggering receptor expressed on myeloid cells 2–deficiency (TRM2)-induced intestinal inflammation and the activation of T cells by an anti-PD1 treatment.[32] Further, this study showed that gavage with *RG* promoted tumor elimination by recruiting inflammatory $CD4^+$ T cells to the tumor. In both this tumor model and our lupus-prone model, inflammation expanded *RG* populations, which then promoted $CD4^+$ T cell activation. We showed here that *RG* expansion featured among the alterations induced by high dietary Trp within the TC microbiota, and these alterations induced autoimmune responses in mice with an inherently normal immune system. These recipient mice also displayed an inflammatory response in the gut, where intestinal microbiota directly encounters dietary Trp. These results suggest that a combination of factors within the gut microbiota of lupus-prone mice and dietary Trp expands *RG* representation in the community, in association with autoimmune activation and inflammation. Furthermore, Trp enhanced *RG2* but not *RG1* strain growth, which was associated with higher level pyrimidine synthesis, a critical factor for bacterial growth,[33] and therefore may contribute to *RG2*'s ability to colonize TC mice. *RG1* and *RG2* also processed Trp differently to produce metabolites that have been shown to have immunomodulatory functions.[34]

Trp has now been implicated in gut microbiome-mediated exacerbations of autoimmune diseases in mouse models of lupus,[9,10] multiple sclerosis (MS),[35,36] and rheumatoid arthritis.[37] In addition, microbiota-induced kynurenic acid expanded proinflammatory Th17-inducing $GPR35^+Ly6C^+$ macrophages in a murine model of MS,[36] and indole promoted the differentiation of Th17 cells that exacerbates collagen-induced arthritis.[37] Hence, Trp metabolites may contribute to inflammation, individually or in combination. Other Trp metabolites such as tryptamine and serotonin have been implicated in inflammatory bowel syndrome in direct association with *RG* abundance.[38,39] We showed here that *RG2* produced high levels of tryptamine and IAAld in the presence of high Trp. Tryptamine, which is naturally more abundant in TC than in B6 control mice, activated mechanistic target of rapamycin (mTOR) and glycolysis in $CD4^+$ T cells.[10] IAAld suppressed the generation of Treg cells, leading to gut inflammatory disorders.[40] Our study uncovered Trp metabolism as a mechanism for *RG* expansion in lupus-prone mice and suggests that Trp metabolites may be involved in its pathogenicity.

Overall, our study suggests a synergistic pathogenic effect between the gut microbiome that develops in an autoimmune environment and the influence of dietary Trp. We propose that this synergistic effect includes the expansion of *RG2*, a candidate pathobiont strain akin to those represented in patients with SLE with high disease activity, which herein is shown to enhance autoimmune activation on a genetically susceptible background. Validation of this hypothesis in other lupus-prone mouse models would support that targeted *RG* depletion or Trp metabolism may improve lupus outcomes.

ACKNOWLEDGMENTS

We thank Dr Tim Garrett and the staff of the University of Florida South East Center for Integrated Metabolomics (SECIM) for the metabolomic analysis, as well as the staff from the Flow Cytometry Shared Resource and the Center for Mucosal and Microbiome Biology at University of Texas Health Science Center at San Antonio.

AUTHOR CONTRIBUTIONS

All authors contributed to at least one of the following manuscript preparation roles: conceptualization AND/OR methodology, software, investigation, formal analysis, data curation, visualization, and validation AND drafting or reviewing/editing the final draft. As corresponding author, Dr Ma confirms that all authors have provided the final approval of the version to be published, and takes responsibility for the affirmations regarding article submission (eg, not under consideration by another journal), the integrity of the data presented, and the statements regarding compliance with institutional review board/Declaration of Helsinki requirements.

REFERENCES

1. Silverman GJ, Azzouz DF, Gisch N, et al. The gut microbiome in systemic lupus erythematosus: lessons from rheumatic fever. Nat Rev Rheumatol 2024;20(3):143–157.
2. Zegarra-Ruiz DF, El Beidaq A, Iñiguez AJ, et al. A diet-sensitive commensal lactobacillus strain mediates TLR7-dependent systemic autoimmunity. Cell Host Microbe 2019;25(1):113–127.e6.

3. Manfredo Vieira S, Hiltensperger M, Kumar V, et al. Translocation of a gut pathobiont drives autoimmunity in mice and humans. Science 2018;359(6380):1156–1161.
4. Azzouz D, Omarbekova A, Heguy A, et al. Lupus nephritis is linked to disease-activity associated expansions and immunity to a gut commensal. Ann Rheum Dis 2019;78(7):947–956.
5. Azzouz DF, Chen Z, Izmirly PM, et al. Longitudinal gut microbiome analyses and blooms of pathogenic strains during lupus disease flares. Ann Rheum Dis 2023;82(10):1315–1327.
6. Silverman GJ, Deng J, Azzouz DF. Sex-dependent lupus *Blautia (Ruminococcus) gnavus* strain induction of zonulin-mediated intestinal permeability and autoimmunity. Front Immunol 2022;13:897971.
7. Crost EH, Coletto E, Bell A, et al. Ruminococcus gnavus: friend or foe for human health. FEMS Microbiol Rev 2023;47(2):fuad014.
8. Morel L, Croker BP, Blenman KR, et al. Genetic reconstitution of systemic lupus erythematosus immunopathology with polycongenic murine strains. Proc Natl Acad Sci USA 2000;97(12):6670–6675.
9. Choi SC, Brown J, Gong M, et al. Gut microbiota dysbiosis and altered tryptophan catabolism contribute to autoimmunity in lupus-susceptible mice. Sci Transl Med 2020;12(551):eaax2220.
10. Brown J, Abboud G, Ma L, et al. Microbiota-mediated skewing of tryptophan catabolism modulates $CD4^+$ T cells in lupus-prone mice. iScience 2022;25(5):104241.
11. Brown J, Robusto B, Morel L. Intestinal dysbiosis and tryptophan metabolism in autoimmunity. Front Immunol 2020;11:1741.
12. Choi SC, Xu Z, Li W, et al. Relative contributions of B cells and dendritic cells from lupus-prone mice to $CD4^+$ T cell polarization. J Immunol 2018;200(9):3087–3099.
13. Elshikha AS, Ge Y, Brown J, et al. Pharmacologic inhibition of glycolysis prevents the development of lupus by altering the gut microbiome in mice. iScience 2023;26(7):107122.
14. Ma L, Terrell M, Brown J, et al. TLR7/TLR8 activation and susceptibility genes synergize to breach gut barrier in a mouse model of lupus. Front Immunol 2023;14:1187145.
15. Wan S, Zhou Z, Duan B, et al. Direct B cell stimulation by dendritic cells in a mouse model of lupus. Arthritis Rheum 2008;58(6):1741–1750.
16. Choi SC, Titov AA, Abboud G, et al. Inhibition of glucose metabolism selectively targets autoreactive follicular helper T cells. Nat Commun 2018;9(1):4369.
17. Ge Y, Zadeh M, Mohamadzadeh M. Vitamin B12 coordinates ileal epithelial cell and microbiota functions to resist Salmonella infection in mice. J Exp Med 2022;219(7):e20220057.
18. Li S, Park Y, Duraisingham S, et al. Predicting network activity from high throughput metabolomics. PLoS Comput Biol 2013;9(7):e1003123.
19. Theofilopoulos AN, Koundouris S, Kono DH, et al. The role of IFN-gamma in systemic lupus erythematosus: a challenge to the Th1/Th2 paradigm in autoimmunity. Arthritis Res 2001;3(3):136–141.
20. Geginat J, Vasco M, Gerosa M, et al. IL-10 producing regulatory and helper T-cells in systemic lupus erythematosus. Semin Immunol 2019;44:101330.
21. Löfmark S, Edlund C, Nord CE. Metronidazole is still the drug of choice for treatment of anaerobic infections. Clin Infect Dis 2010;50-(suppl 1):S16–S23.
22. Bonelli M, Savitskaya A, Steiner CW, et al. Phenotypic and functional analysis of CD4+ CD25- Foxp3+ T cells in patients with systemic lupus erythematosus. J Immunol 2009;182(3):1689–1695.
23. Tackey E, Lipsky PE, Illei GG. Rationale for interleukin-6 blockade in systemic lupus erythematosus. Lupus 2004;13(5):339–343.
24. Villalta D, Bizzaro N, Bassi N, et al. Anti-dsDNA antibody isotypes in systemic lupus erythematosus: IgA in addition to IgG anti-dsDNA help to identify glomerulonephritis and active disease. PLoS One 2013;8(8):e71458.
25. Fasano A. Zonulin, regulation of tight junctions, and autoimmune diseases. Ann N Y Acad Sci 2012;1258(1):25–33.
26. Maxwell JR, Zhang Y, Brown WA, et al. Differential roles for interleukin-23 and interleukin-17 in intestinal immunoregulation. Immunity 2015;43(4):739–750.
27. Lesker TR, Durairaj AC, Gálvez EJC, et al. An integrated metagenome catalog reveals new insights into the murine gut microbiome. Cell Rep 2020;30(9):2909–2922.e6.
28. Murai M, Turovskaya O, Kim G, et al. Interleukin 10 acts on regulatory T cells to maintain expression of the transcription factor Foxp3 and suppressive function in mice with colitis. Nat Immunol 2009;10(11):1178–1184.
29. Chaudhry A, Samstein RM, Treuting P, et al. Interleukin-10 signaling in regulatory T cells is required for suppression of TH17 cell-mediated inflammation. Immunity 2011;34(4):566–578.
30. Wang S, Wang J, Ma R, et al. IL-10 enhances T cell survival and is associated with faster relapse in patients with inactive ulcerative colitis. Mol Immunol 2020;121:92–98.
31. Zhang SX, Wang J, Chen JW, et al. The level of peripheral regulatory T cells is linked to changes in gut commensal microflora in patients with systemic lupus erythematosus. Ann Rheum Dis 2021;80(11):e177.
32. Di Luccia B, Molgora M, Khantakova D, et al. TREM2 deficiency reprograms intestinal macrophages and microbiota to enhance anti-PD-1 tumor immunotherapy. Sci Immunol 2024;9(95):eadi5374.
33. Turnbough CL Jr, Switzer RL. Regulation of pyrimidine biosynthetic gene expression in bacteria: repression without repressors. Microbiol Mol Biol Rev 2008;72(2):266–300, table of contents.
34. Günther J, Fallarino F, Fuchs D, et al. Editorial: immunomodulatory roles of tryptophan metabolites in inflammation and cancer. Front Immunol 2020;11:1497.
35. Montgomery TL, Künstner A, Kennedy JJ, et al. Interactions between host genetics and gut microbiota determine susceptibility to CNS autoimmunity. Proc Natl Acad Sci USA 2020;117(44):27516–27527.
36. Miyamoto K, Sujino T, Harada Y, et al. The gut microbiota-induced kynurenic acid recruits GPR35-positive macrophages to promote experimental encephalitis. Cell Rep 2023;42(8):113005.
37. Seymour BJ, Trent B, Allen BE, et al. Microbiota-dependent indole production stimulates the development of collagen-induced arthritis in mice. J Clin Invest 2023;134(4):e167671.
38. Zhai L, Huang C, Ning Z, et al. Ruminococcus gnavus plays a pathogenic role in diarrhea-predominant irritable bowel syndrome by increasing serotonin biosynthesis. Cell Host Microbe 2023;31(1):33–44.e5.
39. Zhai L, Xiao H, Lin C, et al. Gut microbiota-derived tryptamine and phenethylamine impair insulin sensitivity in metabolic syndrome and irritable bowel syndrome. Nat Commun 2023;14(1):4986.
40. Wojciech L, Png CW, Koh EY, et al. A tryptophan metabolite made by a gut microbiome eukaryote induces pro-inflammatory T cells. Embo J 2023;42(21):e112963.